First Principles Study of Stability and Electronic Structure of TMH and TMH_2 (TM = Y, Zr, Nb)

S. Kanagaprabha[a], A.T. Asvinimeenaatci[b], G. Sudhapriyanga[b], A. JemmyCinthia[b], R. Rajeswarapalanichamy[b,*] and K. Iyakutti[c]

[a]Kamaraj College, Tuticorin, Tamil nadu-628003, India

[b]N.M.S.S. Vellaichamy Nadar College, Madurai, Tamil nadu-625019, India

[c]SRM University, Chennai, Tamil Nadu-603203, India

(Received April 20, 2012; in final form August 30, 2012)

First principles calculations are performed by using Vienna *ab initio* simulation package within the framework of density functional theory to understand the electronic and structural properties of yttrium, zirconium and niobium hydrides. The equilibrium lattice constant, the bulk modulus, the total density of states and charge density distribution are analyzed in comparison with the available experimental and theoretical data. The X-ray diffraction pattern is also simulated to estimate the lattice constants of these hydrides. The formation energies are computed for rock-salt and fluorite structures using density functional theory. The calculated elastic constants obey the necessary stability conditions. A detailed analysis of the changes in density of states and electron density upon hydride formation has allowed us to understand the formation of these hydrides.

DOI: 10.12693/APhysPolA.123.126

PACS: 71.20.Be, 71.15.Mb, 73.20.At, 62.20.de

1. Introduction

Metal hydrides have been attracting the attention of researchers for decades as a hydrogen storage material. Their physical properties are interesting from both fundamental and practical point of view. For example, the hydrogen density in metal hydrides can be larger than that in liquid hydrogen [1]. This interesting fact led to the idea to consider metal hydrides as potential candidates for portable fuel cell applications [2]. However, hydrogen stored in metals causes drastic micro structural changes in the host metallic matrix which can lead to undesirable changes in physical and mechanical properties of a material, such as embrittlement. The mechanism of such embrittlement is believed to be different depending on whether stable hydrides can be formed or not [3].

Hydrides for hydrogen storage need to be able to form hydrides with high hydrogen to metal ratio, but should not be too stable, so that the hydrogen can easily be released without excessive heating. Understanding the stability of metal hydrides is the major key to investigate and design potential hydrogen storage materials. This motivated us to investigate the electronic structure, mechanical stability and storage capacity of transition metal hydrides (TMH and TMH_2, where TM = Y, Zr, and Nb). All the transition metals form a monohydride with the rocksalt structure and dihydride with fluorite structure. Among the transition metals, mainly the $4d$ transition metals form stable hydrides.

In the present work, the density of states (DOS), charge density distribution, and mechanical stability are computed for yttrium, zirconium, and niobium hydrides using VASP code. The X-ray diffraction pattern is also simulated using crystal diffraction software and the lattice constants are determined.

2. Computational details

The quantum mechanical calculations have been performed in the framework of density functional theory using the generalized gradient approximation (GGA) [4, 5] as implemented in the VASP code [6, 7]. The interaction between the ion and electron is described by the projector augmented wave method [8]. The cutoff energy for plane waves in our calculation is 400 eV for each solid. The Birllouin-zone integrations are performed on the Monkhorst–Pack K-point mesh [9]. For medium sized cells ($12 \times 12 \times 12$) K-point meshes were used for all the $4d$ transition metal hydrides. The Wigner–Seitz sphere was chosen in such a way that the boundary potential was minimum and charge flow between the atoms was in accordance with the electronegativity criteria. The E and K convergence are also checked. The tetrahedron method [10, 11] of the Brillouin zone integration is used to calculate the total density of states. The total energy was computed by changing the volume from 1.0 to $0.5V_0$, where V_0 is the equilibrium cell volume.

3. Results and discussion

3.1. Geometric property

At ambient condition the yttrium, zirconium, and niobium hydrides crystallize in rocksalt structure with the space group $Fm3m$ (225). In the unit cell of TMH (TM = Y, Zr, Nb) the transition metal atoms are positioned

*corresponding author; e-mail: rrpcaspd2003@gmail.com

at 4a:$(0,0,0)$ and H atom at 4b:$(0.5,0.5,0.5)$ and contains four formula units per unit cell. But in the case of dihydrides with fluorite structure, the H atoms are positioned at $(0.25,0.25,0.25)$. The primitive unit cell of mono and dihydrides of yttrium, zirconium, and niobium with rock-salt and fluorite structure is shown in Fig. 1.

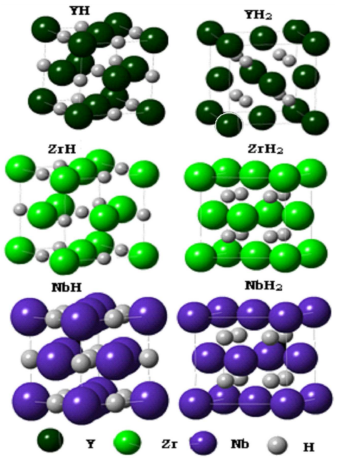

Fig. 1. The primitive unit cell of mono- and dihydrides of yttrium, zirconium, and niobium with rock-salt and fluorite.

3.2. Stability of TMH and TMH_2 and formation energy

The stability of metal hydrides (TMH and TMH_2, TM = Y, Zr, and Nb) is analyzed by computing the formation energy using the following relation:

$$\Delta H_1 = E_{\rm tot}({\rm TMH}) - E_{\rm tot}({\rm TM}) - (1/2)E_{\rm tot}({\rm H_2}), \tag{1}$$

$$\Delta H_2 = E_{\rm tot}({\rm TMH_2}) - E_{\rm tot}({\rm TM}) - E_{\rm tot}({\rm H_2}), \tag{2}$$

where $E_{\rm tot}({\rm TMH_2})$ and $E_{\rm tot}({\rm TMH})$ are the energies of primitive cells of TMH_2 and TMH, respectively. $E_{\rm tot}({\rm TM})$ and $E_{\rm tot}({\rm H_2})$ are the energies of a transition metal atom and a hydrogen molecule. The energy of the metal and metal hydride is calculated using VASP code, performed in the framework of density functional theory using the GGA. The value of heat of formation ΔH for mono and dihydrides are calculated using Eq. (1) and Eq. (2), respectively. The variation of heat of formation for yttrium, zirconium, and niobium monohydride with rocksalt structure and dihydride with fluorite structure are shown in Fig. 2. The trends in both mono and dihydrides are quite similar and common. From Fig. 2, it is observed that the stability of the hydride rapidly increases as we move from yttrium to niobium. Figure 3 offers a further illustration of the importance of the valence electron count for the chemical hydrogen insertion energy. It shows the chemical component of the hydrogen insertion energy as function of the number of valence electrons $(s+d)$ for the hydrides in both the fluorite (MH_2) and rock-salt (MH) structures.

The computed lattice parameter a_0 [Å], equlibrium cell volume V_0 [Å^3], valence electron density ρ [electrons/Å^3],

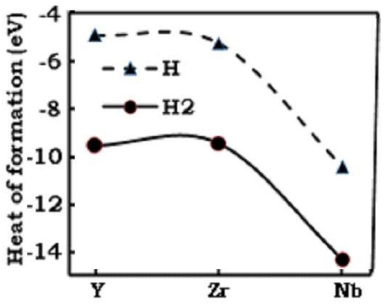

Fig. 2. Formation energy for the monohydrides (a) and dihydrides (b) of yttrium, zirconium, and niobium metals.

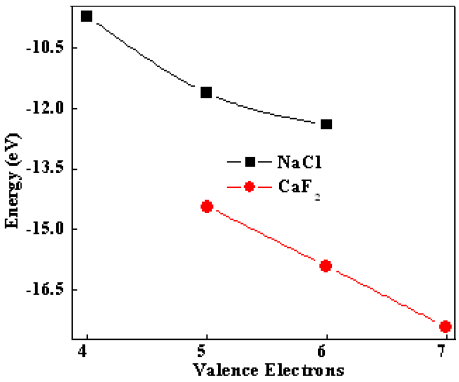

Fig. 3. Chemical contributions to the hydride formation energy as function of the number of valence electrons (energy given per H_2 molecule).

bulk modulus B_0 [GPa] and its derivative B_0' for the hydride in rock-salt and fluorite structures are given in Table I along with available experimental data [12–15]. Valence electron density (VED) is defined as the total number of valence electrons divided by volume per unit cell. The calculated valence electron density for niobium hydrides is greater than that of yttrium and zirconium hydrides.

TABLE I

Calculated lattice parameters a_0 [Å], cell volume V_0 [Å^3], valence electron density ρ [electrons/Å^3], bulk modulus B_0 [GPa] and its pressure derivative B_0' for the yttrium, zirconium, and niobium metal hydrides in the rocksalt (NaCl) and fluorite (CaF_2) structures.

	Y		Zr		Nb	
	H	H_2	H	H_2	H	H_2
a_0	4.429	5.129	5.139	4.717	3.430	4.340
		5.203 [12]		4.78 [13]	3.445 [15]	4.566 [14]
V_0	21.72	26.4	33.93	21.55	17.23	20.44
ρ	0.184	0.189	0.147	0.278	0.348	0.342
B_0	227	108	332	212	245	201
		101 [16]		152 [16]		198 [16]
B_0'	2.790	3.562	3.395	4.37	3.034	4.721

The simulated X-ray diffraction (XRD) pattern of yttrium, zirconium, and niobium monohydride with NaCl

structure and dihydride with CaF_2 structure is shown in Fig. 4a–c. A monochromatic radiation of wavelength 1.5406 Å is used to simulate the XRD pattern. The diffraction peaks are obtained using the Lorentz function. The sharp, narrow diffraction peaks show the absence of impurity in the simulated structures. The lattice parameter is calculated using the expression

$$a = d_{hkl} \times \sqrt{h^2 + k^2 + l^2}. \quad (3)$$

The calculated lattice parameters for YH is 4.428 Å (111 plane), YH_2 is 5.128 Å (111 plane), ZrH is 5.138 Å (111 plane), ZrH_2 is 4.716 Å (111 plane), NbH is 3.43 Å (002 plane) and NbH_2 is 4.338 Å (022 plane), which are in good agreement with the available experimental and theoretical data [12–15]. The electronic DOS for yttrium, zirconium, and niobium are shown for metal in Fig. 5, for monohydride in Fig. 6, and for dihydrides with CaF_2 structure in Fig. 7.

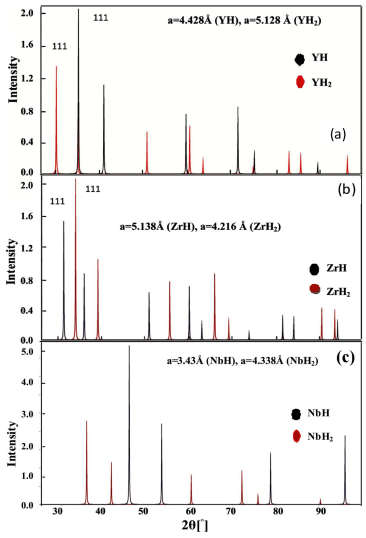

Fig. 4. The simulated XRD pattern of TMH and TMH_2 (TM = Y, Zr, Nb).

The valence state of yttrium, zirconium and niobium hydrides are due to $4d^15s^2$ of Y, $4d^25s^2$ of Zr, $4d^45s^1$ of Nb and $1s^1$ state electrons of hydrogen atom, respectively. In the monohydrides, the hydrogen character is isolated within the lowest peak, which is a single occupied band holding two electrons. This lowest band possesses significant hydrogen character, in addition to a characteristic free electron tail and some metal character. Along the series, the number of electrons in the d-state increases steadily with the increase in the atomic number. The states between −5 eV and 5 eV are dominated by yttrium and niobium metal (M) -s states with a small contribution from the hydrogen atom, but in the case of niobium it is different. The states above −5 eV are mainly composed of M ($4d$) states and H $1s$ state. These results indicate a strong hybridization between the H $1s$ and M d states. The central part of the DOS is characterized by two regions. The lower region arises from the

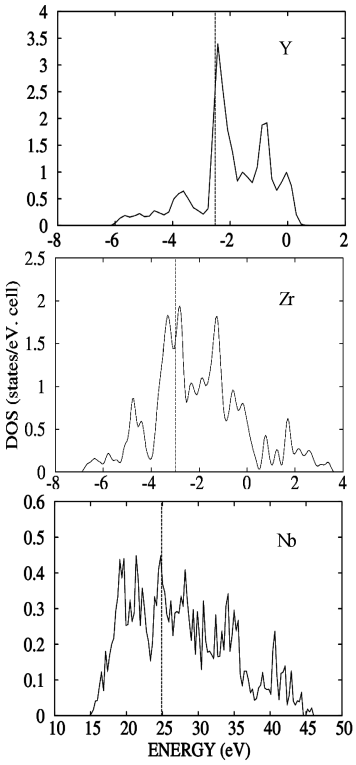

Fig. 5. Total density of states (DOS) for Y, Zr, and Nb in the fcc structure.

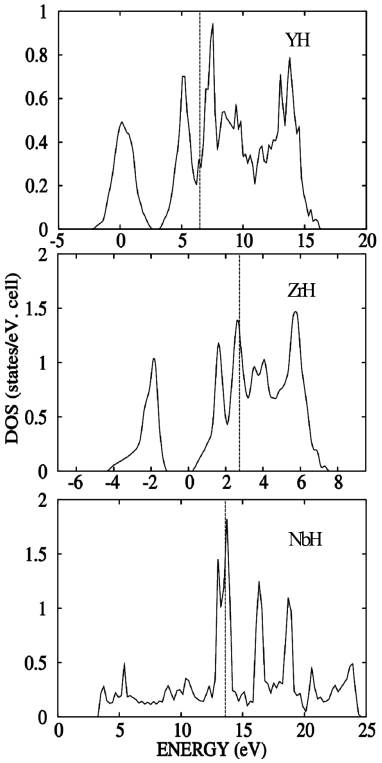

Fig. 6. Total density of states (DOS) for YH, ZrH, and NbH in the rocksalt structure.

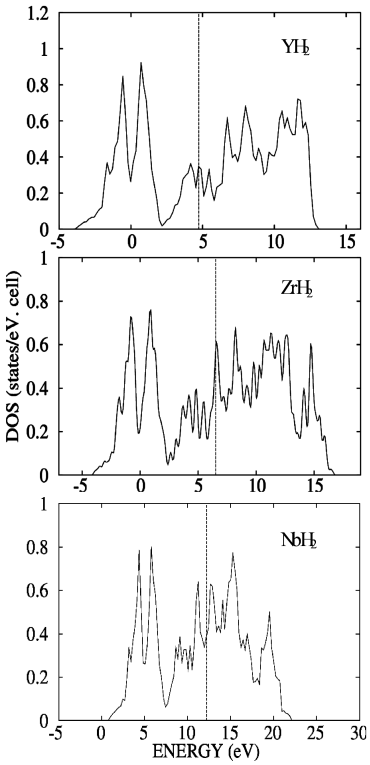

Fig. 7. Total density of states (DOS) for YH_2, ZrH_2, and NbH_2 in the fluorite structure.

hybridization of p and d states of the transition metal, and the upper region is highly dominated by $4d$ states. The valence states are separated by a wide gap from the occupied states, indicating covalent behavior. Above the Fermi level the empty conduction states are present with a mixed s, p, and d characters. Therefore at ambient pressure all these three hydrides show metallic behavior.

The charge density distribution for TMH and TMH_2 (TM = Y, Zr, Nb) containing TM^+ and H^- ion is shown in Fig. 8. From Fig. 8, it is observed that the voids (i.e. charge depletion regions) are narrow between H ions and broad between the yttrium ions. On increasing the TM--ion atomic number the TM–H bonding becomes stronger and these voids change their shape. It is also found that the light colored areas indicate electron gain, whereas the darker areas indicate electron loss. Because the electron gain on hydrogen is so much greater than on the transition metal, the minimum and maximum values of electron gain and loss were truncated, in order to keep enough resolution around the transition metals. Electron gain on the hydrogen position is substantial, indicating that the hydrogen does not insert as a bare proton. Near the transition metal there are both regions of positive and negative charge difference, corresponding to the loss or gain of d occupation. Significant loss off d state electrons is observed, which is due to the formation of a bonding-antibonding pair between the directly overlapping of hydrogen s with metal d orbitals. A more detailed

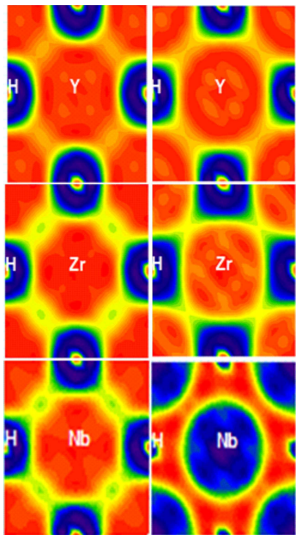

Fig. 8. Charge density distributions for yttrium, zirconium, and niobium mono- and dihydrides.

understanding of which d orbital's gain occupation can be obtained from the total density of states.

3.3. Mechanical property

The calculated elastic constants yttrium, zirconium, and niobium monohydride (rock-salt structure) and dihydride (fluorite structure) are presented in Table II. For a stable cubic crystal, the three independent elastic constants C_{ij} (C_{11}, C_{12}, C_{44}) should satisfy the well known Born–Huang criteria for the stability of cubic crystals [17]:

$$C_{44} > 0, \quad C_{11} > |C_{12}|, \quad C_{11} + 2C_{12} > 0. \tag{4}$$

It is found that the elastic constants obtained for cubic transition metal hydrides satisfy the Born–Huang criteria, suggesting that they are mechanically stable. Young's modulus E and Poisson's ratio are the two important factors for technological and engineering applications. The stiffness of the solid can be analyzed using the Young modulus (E) value. The Young modulus E and Poisson ratio υ are calculated using the expression

$$E = 9BG/(3B + G), \tag{5}$$

$$\upsilon = (3B - 2G)/\left[2(3B + G)\right]. \tag{6}$$

Bulk modulus B_0 [GPa], Young's modulus E [GPa], shear modulus G [GPa], Poisson's ratio υ and the elastic constants C_{11}, C_{12}, and C_{44} are calculated and are given in Table II. It is found that the Young modulus of ZrH_2 is 316 GPa which is greater than that of YH_2 and NbH_2. It shows that ZrH_2 is stiffer than yttrium and niobium hydride. Poisson's ratio reflects the stability of the crystal against shear. The ratio can formally take value between -1 and 0.5, which corresponds to the lower limit where the material does not change its shape or to the upper when the volume remains unchanged.

TABLE II

Calculated elastic constants C_{11}, C_{12}, C_{44} [GPa], Young's modulus E [GPa], shear modulus G [GPa] and Poisson's ratio υ for yttrium, zirconium, and niobium mono- and dihydrides.

	Y		Zr		Nb	
	H	H_2	H	H_2	H	H_2
C_{11}	373	230	486	250	362	209
C_{12}	155	48.3	255	87	187	97
C_{44}	108	90.8	116	82	88	56
E	279	212	316	218	235	154
G	108	90.8	116	82	88	56
ϵ	0.29	0.17	0.34	0.25	0.34	0.31

3.4. Hydrogen storage in TMH and TMH_2

Hydrogen fuel, which can be readily produced from renewable energy sources, contains at least three times larger chemical energy per mass $\approx$ 142 MJ kg^{-1} than any chemical fuel, thus making a hydrogen fuel cell an attractive alternative to an internal combustion engine for transportation. Elements, especially those in groups I–IV and some transition metals, have their hydride and amide/imide forms. There is, therefore, still plenty of scope for further exploring metal–H systems for hydrogen storage. In our study, we have analyzed the storage capacity of yttrium, zirconium, and niobium hydrides. Formation energy per unit volume (eV) and weight percentage of hydrogen for yttrium, zirconium, and niobium are computed and are given in Table III. The maximum storage capacity is found to be 3.28% in YH_3. Our results conclude that the hydrogen storage capacity decreases as we move from yttrium (Y) to niobium (Nb).

TABLE III

Storage capacity of hydrogen in yttrium, zirconium, and niobium metals.

	Formation energy/unit volume [eV]	[wt%] of hydrogen
YH	−4.878	1.12
YH_2	−9.532	2.21
YH_3	−98.631	3.28
ZrH	−5.216	1.09
ZrH_2	−9.410	2.16
ZrH_3	−94.613	3.20
NbH	−10.422	1.07
NbH_2	−14.298	2.12
NbH_3	−95.536	3.15

From the density of states, it is also observed that the s-state electrons of the hydrogen atoms contribute more near the Fermi level. Therefore it is easy to release the hydrogen atoms. Thus our results indicate that among the $4d$ transition metal mono-, di- and trihydrides, YH_3 is one of the best hydrogen storage materials with the storage capacity of 3.28%.

4. Conclusion

The electronic structure and mechanical stability for the yttrium, zirconium, and niobium hydrides are investigated based on first principles calculation under the frame work of density functional theory using the GGA. Our results suggest that all the yttrium, zirconium and niobium hydrides are mechanically stable in the rocksalt and fluorite structure. It is found that the bonding in these hydrides is a mixture of metallic and covalent characters. Among the hydrides considered, YH_3 is found to be one of the best hydrogen storage material and the maximum storage capacity achieved in YH_3 is 3.28%.

Acknowledgments

We thank our college management for their constant encouragement. The financial assistance from UGC (MRP.F.No.38-141/2009), India is duly acknowledged.

References

[1] M.J. Latroche, *Phys. Chem. Solids* **65**, 517 (2004).

[2] R. Viswall, G. Alefeld, *Hydrogen Storage in Metals II*, Springer, Berlin 1978, p. 201.

[3] H. Vehoff, in: *Hydrogen in Metals III, Properties and Applications*, Ed. H. Wipf, Springer-Verlag, Berlin 1997, p. 215.

[4] Z.A. Schlapbach, *Nature (London)* **414**, 353 (2001).

[5] J. Perdew, J.A. Chevary, S.H. Vosko, K.A. Jackson, M.R. Pederson, D.J. Singh, C. Fiolhais, *Phys. Rev. B* **46**, 6671 (1992).

[6] J. Perdew, A. Zunger, *Phys. Rev. B* **23**, 5048 (1981).

[7] G. Kresse, J. Furthmuller, *Comput. Mater. Sci.* **6**, 15 (1996).

[8] G. Kresse, J. Furthmuller, *Phys. Rev. B* **54**, 11169 (1996).

[9] P.E. Blochl, *Phys. Rev. B* **17**, 17953 (1994).

[10] H.J. Monkhorst, J.D. Pack, *Phys. Rev. B* **13**, 5188 (1976).

[11] O.K. Anderson, *Phys. Rev. B* **12**, 3060 (1975).

[12] J.N. Daou, P. Vajda, *Phys. Rev. B* **45**, 10907 (1992).

[13] F. Ducastelle, R. Caudron, P. Costa, *J. Phys. (France)* **31**, 57 (1970).

[14] H. Muller, K. Weymann, *J. Less-Common Met.* **119**, 15 (1986).

[15] Vipul Strivatsa, M. Rajagopalan, *J. Magn. Magn. Mater.* **321**, 607 (2009).

[16] W. Wolf, P. Herzig, *J. Condens. Matter Phys.* **12**, 4535 (2000).

[17] M. Born, K. Huang, *Dynamical Theory of Crystal Lattices*, Clarendon, Oxford 1956.

[1] M.J. Latroche, *Phys. Chem. Solids* **65**, 517 (2004).

[2] R. Viswall, G. Alefeld, *Hydrogen Storage in Metals II*, Springer, Berlin 1978, p. 201.

[3] H. Vehoff, in: *Hydrogen in Metals III, Properties and Applications*, Ed. H. Wipf, Springer-Verlag, Berlin 1997, p. 215.

[4] Z.A. Schlapbach, *Nature (London)* **414**, 353 (2001).

[5] J. Perdew, J.A. Chevary, S.H. Vosko, K.A. Jackson, M.R. Pederson, D.J. Singh, C. Fiolhais, *Phys. Rev. B* **46**, 6671 (1992).

[6] J. Perdew, A. Zunger, *Phys. Rev. B* **23**, 5048 (1981).

[7] G. Kresse, J. Furthmuller, *Comput. Mater. Sci.* **6**, 15 (1996).

[8] G. Kresse, J. Furthmuller, *Phys. Rev. B* **54**, 11169 (1996).

[9] P.E. Blochl, *Phys. Rev. B* **17**, 17953 (1994).

[10] H.J. Monkhorst, J.D. Pack, *Phys. Rev. B* **13**, 5188 (1976).

[11] O.K. Anderson, *Phys. Rev. B* **12**, 3060 (1975).

[12] J.N. Daou, P. Vajda, *Phys. Rev. B* **45**, 10907 (1992).

[13] F. Ducastelle, R. Caudron, P. Costa, *J. Phys. (France)* **31**, 57 (1970).

[14] H. Muller, K. Weymann, *J. Less-Common Met.* **119**, 15 (1986).

[15] Vipul Strivatsa, M. Rajagopalan, *J. Magn. Magn. Mater.* **321**, 607 (2009).

[16] W. Wolf, P. Herzig, *J. Condens. Matter Phys.* **12**, 4535 (2000).

[17] M. Born, K. Huang, *Dynamical Theory of Crystal Lattices*, Clarendon, Oxford 1956.